Conformation and Dynamics of the SH1−SH2 Helix in Scallop Myosin[†]

Lisa K. Nitao,[‡] Rachel R. Ogorzalek Loo,[‡,§] Elizabeth O'Neall-Hennessey,[||] Joseph A. Loo,[‡,§] Andrew G. Szent-Györgyi,[||] and Emil Reisler*[,‡]

Department of Chemistry and Biochemistry and the Molecular Biology Institute and Department of Biological Chemistry, University of California, Los Angeles, California 90095, and Department of Biology and the Rosentiel Basic Medical Sciences Research Center, Brandeis University, Waltham, Massachusetts 02454

Received December 5, 2002; Revised Manuscript Received April 8, 2003

ABSTRACT: Atomic structures of scallop myosin subfragment 1(S1) with the bound MgADP, MgAMPPNP, and MgADP·BeF_x provide crystallographic evidence for a destabilization of the helix containing reactive thiols SH1 (Cys703) and SH2 (Cys693). A destabilization of this helix was not observed in previous structures of S1 (from chicken skeletal, *Dictyostelium discoideum*, and smooth muscle myosins), including complexes for which solution experiments indicated such a destabilization. In this study, the factors that influence the SH1−SH2 helix in scallop S1 were examined using monofunctional and bifunctional thiol reagents. The rate of monofunctional labeling of scallop S1 was increased in the presence of MgADP and MgATPγS but was inhibited by MgADP·V_i and actin. The resulting changes in ATPase activities of S1 were symptomatic of SH2 and not SH1 modification, which was confirmed by mass spectrometry analysis. With bifunctional reagents of various lengths, cross-linking did not occur on a short time scale in the absence of nucleotides. In the presence of MgADP, cross-linking was greatly enhanced for all of the reagents. These reactions, as well as the formation of a disulfide bond between SH1 and SH2, were much faster in scallop S1·ADP than in rabbit skeletal S1·ADP and were rate-limited by the initial attachment of the reagent to scallop S1. The cross-linking sites were mapped by mass spectrometry to SH1 and SH2. These results reveal isoform-specific differences in the conformation and dynamics of the SH1−SH2 helix, providing a possible explanation for destabilization of this helix in some scallop S1 but not in other S1 isoform structures.

Myosin is a molecular motor that utilizes the chemical energy of ATP to generate force for muscle contraction and drives many cellular functions in nonmuscle cells. As ATP is hydrolyzed, myosin is believed to undergo conformational changes in the catalytic domain, which lead to the swinging of the lever arm. In an attempt to map these changes, the myosin head has been crystallized in several different nucleotide states, using different isoforms of myosin (*1*−*9*). From the comparison of these different structures, it was proposed that three structural elements acting as joints coordinate the movements of the four subdomains within the myosin head (*8*). These joints (relay, SH1[1] helix, switch II) direct the overall organization of the myosin head and the transmission of conformational changes between its different regions.

One of the notable features of several scallop S1 (S1·ADP, S1·AMPPNP, S1·ADP·BeF_x) structures is the conformation of one of its joints, the SH1−SH2 helix (*7*, *9*). This is the first isoform of S1 with a disordered SH1−SH2 helix, which corresponds to what has been observed for many years in solution biochemical studies on other isoforms of S1. In solution, nucleotides destabilize the SH1−SH2 helix of skeletal S1, which allows SH1 and SH2 to be cross-linked readily by reagents with spans of 3−14 Å (*10*, *11*). Direct evidence for nucleotide-induced motions in this region was also obtained from measurements of the rotational mobility of spin probes attached to SH1 (*12*, *13*). Functional significance of the dynamic properties of the helix was demonstrated in recent studies in which mutations of key glycine

[†] This work was supported by USPHS Grant AR22301, National Science Foundation Grant MCB 9904599 (to E.R.), and U.S. Department of Energy Grant to the UCLA Laboratory of Genomics and Proteomics (DE-FC03-87ER60615) (to J.A.L.). The mass spectrometry equipment was supplied by the generous gift from the W. M. Keck Foundation. Dr. Andrew Szent-Györgyi was supported in part by NIH Grant AR17346 to Dr. C. Cohen.

* To whom correspondence should be addressed. E-mail: reisler@mbi.ucla.edu.

[‡] Department of Chemistry and Biochemistry and the Molecular Biology Institute, University of California, Los Angeles.

[§] Department of Biological Chemistry, University of California, Los Angeles.

[||] Brandeis University.

[1] Abbreviations: AlF_4^-, aluminum fluoride; ATPγS, adenosine 5′-(3-thiotriphosphate); BeF_x, beryllium fluoride; BM, 1,1′-(methylenedi-4,1-phenylene) bismaleimide; DMF, dimethylformamide; DTNB, 5,5′-dithio-bis-(2-nitrobenzoic acid); DTT, dithiothreitol; ESI, electrospray ionization; HCCA, α-cyano-4-hydroxy-cinnamic acid; IAEDANS, *N*-(iodoacetyl)-*N*′-(5-sulfo-1-naphthyl)ethylenediamine; IAA, iodoacetic acid; LC-ESI-MS/MS, liquid chromatography-electrospray ionization-mass spectrometry-mass spectrometry; MALDI, matrix-assisted laser desorption/ionization; MD, motor domain; mPDM, *N*,*N*′-1,3-phenylene dimaleimide; MS, mass spectrometry; *m*/*z*, mass-to-charge ratio; NEM, *N*-ethylmaleimide; NTB, 2-nitro-5-thiobenzoic acid; oPDM, *N*,*N*′-1,2-phenylene dimaleimide; pQ, pyro-glutamyl; pPDM, *N*,*N*′-1,4-phenylenedimaleimide; S1, myosin subfragment 1; SH1, Cys707 or Cys703 of the rabbit skeletal or scallop S1 sequence, respectively; SH2, Cys697 or Cys693 of rabbit or scallop S1; TFA, trifluoroacetic acid; V_i, vanadate.

10.1021/bi027312u CCC: $25.00
Published on Web 06/05/2003

residues in the helix to alanines (*14*, *15*) and SH1 or SH2 labeling (*16*−*19*) resulted in a complete loss of the myosin motor function. Yet, all previous structures show this helix in a rigid conformation, with the SH1 and SH2 groups being approximately 19 Å apart (*1*, *2*, *4*−*6*). In the scallop S1·ADP structure, the SH1 portion of the helix is collapsed, allowing SH1 and SH2 to approach within ∼7 Å of each other (*7*). Because of the disordered helix, the open actin binding cleft, and the unique positioning of the converter and lever arm, the scallop S1·ADP crystal structure was proposed to represent the structure of the weakly bound S1·ATP state (*7*). Notably, the recent structures of scallop S1·AMPPNP and S1·ADP·BeF_x are indeed analogous to the S1·ADP structure, containing the destabilized SH1−SH2 helix (*9*).

One question concerning the different structures is why scallop S1 crystallizes in an ATP-like state with a melted SH1−SH2 helix, in contrast to ATP-like states (i.e., S1·ATPγS, S1·ADP·BeF_x, and S1·AMP·PNP) of other isoforms of S1. Because different myosin isoforms have different mechanical properties, small sequence and structural differences may provide the basis for their functional variability. In some cases, truncation of S1 may also be affecting the stability the SH1−SH2 helix. Thus, the conformation and dynamics of the SH1−SH2 helix region may be different in scallop S1 than in other S1 isoforms. Such a possibility is indicated by the recent crystallographic mapping of the pPDM cross-linking in scallop S1 to the SH2 (Cys693) and Lys705 residues (*9*). However, little, if any, information exists about the solution properties of the SH1−SH2 region in scallop S1.

The focus of this study has been to investigate the dynamics of the SH1−SH2 helix region in scallop S1. To do so, we employed monofunctional and bifunctional thiol reagents to modify SH1 and SH2 in different states of scallop S1. The results obtained with NEM indicate that the modification of scallop S1, like that of skeletal S1, is affected by the presence of actin and nucleotides. Similar experiments with the SH1-specific (in skeletal S1) reagent, IAEDANS, combined with mass spectrometry of the labeled scallop S1 identified the site of IAEDANS modification to the SH2 and not the SH1 group. Our results with bifunctional reagents indicate that the cross-linking reaction occurs slowly, if at all, in the nucleotide-free state of scallop S1. In the MgADP and MgATPγS states of scallop S1, modification reactions occur very quickly for every reagent (∼7−15 Å) that was used. These cross-linkings and disulfide bond formation are rate-limited by the initial attachment of the reagent to scallop S1. Cross-linking was strongly inhibited in the MgADP·V_i state. Mass spectrometric analysis of pPDM cross-linked scallop S1 and ATPase measurements confirmed that the cross-linking occurs from SH2 to SH1. These results show that the local conformation and dynamics of the SH1−SH2 helix region in scallop S1 are different than in skeletal S1. The lower stability of the scallop SH1−SH2 helix may account for the disordered state observed in several scallop S1−nucleotide structures.

EXPERIMENTAL PROCEDURES

Reagents. *N*-Ethylmaleimide (NEM), *N*,*N*′-1,3-phenylene dimaleimide (mPDM), 1,1′-(methylenedi-4,1-phenylene) bismaleimide (BM), 5,5′-dithiobis(2-nitrobenzoic acid) (DTNB), IAA (iodoacetic acid), ADP, soybean trypsin inhibitor, Sephadex G-50, sinapinic acid, and α-cyano-4-hydroxycinnamic acid (HCCA) were purchased from Sigma-Aldrich (St. Louis, MO). *N*,*N*′-1,2-Phenylene dimaleimide (oPDM) and *N*,*N*′-1,4-phenylene dimaleimide (pPDM) were purchased from Research Organics (Cleveland, OH). *N*-(Iodoacetyl)-*N*′-(5-sulfo-1-naphthyl)ethylenediamine (IAEDANS) was obtained from Molecular Probes (Eugene, OR). Adenosine-5′-(3-thiotriphosphate) (ATPγS) was obtained from Boehringer Mannheim (Germany). Sequencing grade modified trypsin was obtained from Promega (Madison, WI).

Proteins. Skeletal actin and myosin were obtained from rabbit back and leg muscles as described previously (*20*, *21*). Subfragment-1 (S1) was prepared from the chymotryptic digestion of myosin filaments (*22*). The concentration of skeletal S1 and actin was determined spectrophotometrically by using the extinction coefficients of $E^{1\%}_{280} = 7.5\ cm^{-1}$ and $E^{1\%}_{292} = 11.5\ cm^{-1}$, respectively. Unless otherwise noted, all experiments with skeletal S1 were performed in 40 mM KCl, 10 mM PIPES, pH 7.0. NEM-modified actin (at Cys374) was prepared by adding a 10-fold excess of NEM to G-actin for 3 h at 4 °C. The reaction was stopped with the addition of 1.0 mM DTT. The extent of modification of Cys374 was determined by monitoring the loss of quenching of tryptophan fluorescence by Cu^{2+}, as described previously (*23*). Under these conditions, approximately 95% of the actin was modified (data not shown). As described previously, scallop myosin was obtained from the striated muscle of *Argopecten irradians* (*24*) and digested with affinity-purified papain to obtain S1 (*25*, *26*). The concentration of scallop S1 was determined by using an extinction coefficient of $E^{1\%}_{280} = 8.0\ cm^{-1}$. Unless otherwise noted, all experiments involving scallop S1 were performed in a buffer containing 100 mM NaCl, 20 mM MOPS (pH 7.0), 2.0 mM $MgCl_2$, 0.1 mM EDTA, and 0.2 mM $CaCl_2$.

ATPase Activity Determinations. As described previously, Ca^{2+}− and EDTA (K^+)−ATPase activities of skeletal S1 were determined at 37 °C (*27*). For scallop S1, the measurements were made at 25 °C. The Ca^{2+}−ATPase assay solution contained 600 mM KCl, 50 mM Tris-HCl (pH 7.8), 5.0 mM $CaCl_2$, and 2.0 mM ATP. The EDTA−ATPase assay solution contained 444 mM KCl, 50 mM histidine, 50 mM Tris-HCl (pH 7.8), 5.0 mM EDTA, and 2.0 mM ATP.

Preparation of S1 Complexes with BeF_x and AlF_4^- and V_i. The complexes of unmodified and modified S1 with phosphate analogues were formed by incubation of 20−30 μM S1 with 1.0 mM MgADP for 10 min and then 5.0 mM NaF + 0.5 mM $BeCl_2$, or 10 mM NaF + 0.5 mM $AlCl_3$, or 1.0 mM NaV_i for 30 min at room temperature. After 30 min, the samples were incubated on ice until use. The extent of complex formation was determined by the loss of EDTA−ATPase or Ca^{2+}−ATPase activity.

Monofunctional Modification Reactions. All modification reactions with skeletal S1 were performed in a buffer containing 40 mM KCl and 10 mM PIPES, pH 7.0. All modifications and preparations of modified scallop were done in buffers containing 100 mM NaCl, 20 mM MOPS (pH 7.0), 2.0 mM $MgCl_2$, 0.1 mM EDTA, and 0.2 mM $CaCl_2$.

NEM Modification. Scallop S1 (8.0 μM) or skeletal S1 (16 μM) was modified with a 4-fold molar excess of NEM

(dissolved in ethanol) in the presence and absence of 1.0 mM nucleotide (MgADP, MgATPγS) and NEM-actin (24 μM) at 4 °C. The modifications were stopped in reaction aliquots with 1.0 mM DTT, and the Ca^{2+}− and EDTA−ATPase activity of each time point was measured to determine the extent of modification. For the reaction in the MgADP·V_i state, the complex was formed, and the excess ADP and V_i was removed on spin columns that were equilibrated with the reaction buffer. The concentration of S1·MgADP·V_i was determined using the Bradford assay (*28*), as modified by Bio-Rad. The extent of the complex formation (at least 95%, data not shown) was determined from the measurements of the Ca^{2+}− and EDTA−ATPase activities of S1. After the addition of NEM, each time point aliquot was quenched with 1.0 mM DTT. To remove the bound MgADP·V_i, a 3-fold molar excess of actin was added. After an overnight incubation of the samples at 4 °C to allow for a complete release of the bound complex, the ATPase activity of each time point was measured to determine the extent of modification. Removal of the ADP·V_i was assessed by measuring the Ca^{2+}− and EDTA−ATPase activities of the initial time point aliquot of the ADP·V_i reaction and comparing those values with those of uncomplexed S1. In all cases, the removal was at least 90% complete.

IAEDANS Modification. Scallop S1 (10 μM) was modified at different molar ratios of IAEDANS (in DMF) to S1. Each reaction took place at 4 °C and was terminated with 1.0 mM DTT after 10 min. The Ca^{2+}− and EDTA−ATPase activity of each reaction was measured to determine the extent of modification.

Cross-Linking of Scallop and Skeletal S1. All modification experiments with skeletal S1 were performed in buffers containing 40 mM KCl and 10 mM PIPES, pH 7.0. For scallop S1, the reaction buffer was comprised of 100 mM NaCl, 20 mM MOPS (pH 7.0), 2 mM $MgCl_2$, 0.2 mM $CaCl_2$, and 0.1 mM EDTA. The preparations of pPDM-modified scallop S1 for use in other experiments were also carried out in this buffer.

In the nucleotide-free state, scallop or skeletal S1 (12 μM) was modified with a 1.5-fold molar excess of cross-linking reagent (oPDM, mPDM, pPDM, or BM in DMF) at 4 °C. In the nucleotide-bound states, scallop or skeletal S1 (10 μM) was modified in the presence of 1.0 mM nucleotide (MgADP or MgATPγS) and a 1.5-fold molar excess of cross-linking reagent (oPDM, mPDM, pPDM, BM). At selected time points, reaction aliquots were quenched with the addition of 1.0 mM DTT. For disulfide bond formation, scallop or skeletal S1 was reacted with a 2-fold molar excess of DTNB in the presence of 1.0 mM MgADP. To stop this reaction, each time point aliquot was spun through a spin column, equilibrated with the reaction buffer, to remove the unreacted DTNB. S1 concentration in each aliquot was determined by the Bradford assay (*28*), as modified by Bio-Rad. The Ca^{2+}− and EDTA−ATPase activities of each aliquot were measured to determine the extent of modification/disulfide bond formation. For the cross-linking reaction in the MgADP·V_i state, the complex was formed as described above and then reacted with pPDM. This reaction was stopped in each time point aliquot with 1.0 mM DTT. The bound ADP·V_i was removed from S1 as described above, and the ATPase activity of each aliquot was measured to determine the extent of modification. The removal of the ADP·V_i was assessed by comparing the Ca^{2+}− and EDTA−ATPase activities of the initial time point aliquot of the ADP·V_i reaction to those of uncomplexed S1. In all cases, the removal was at least 90% complete.

Thiol Titration of Scallop S1 with DTNB. Prior to any DTNB experiment, all samples were run though spin columns equilibrated with 100 mM KCl and 20 mM MOPS, pH 7.0, to remove any DTT. The concentration of S1 was determined by the Bradford assay. Unmodified and modified scallop S1 (3.0 μM) was denatured in 6.0 M urea, 50 mM Tris, pH 8.0 for 15 min at 60 °C. After the samples were cooled to room temperature, DTNB (300 μM) was added to them. After 15 min, the absorbance of the samples was measured at 412 nm, and the amount of unmodified cysteine groups was determined by using a molar extinction coefficient of 14 290 M^{-1} cm^{-1} (*29*).

Cosedimentation Assays. The binding constants of unmodified and modified scallop S1 to skeletal actin were determined using the cosedimentation assay. Scallop S1 (25 μM) was modified for 15 min at 4 °C in the presence of 1.0 mM MgADP by a 2-fold molar excess of cross-linking reagent (oPDM, pPDM, BM). The DTNB reaction time was extended to 90 min, after which the unreacted DTNB was removed on spin columns. The concentration of the modified scallop S1 was determined using the Bradford assay, and the extent of modification was determined via the ATPase activity assay. Under these conditions, at least 90% of the S1 were cross-linked. For the binding experiments, the concentration of S1 was kept constant at 4.0 μM; the concentration of actin varied from 0 to 25 μM (for rigor conditions) or 0 to 100 μM (for cross-linked S1 or S1 complexed with ADP·BeF_x). The samples of S1 were incubated with F-actin for 30 min at room temperature and then spun in a Beckman airfuge for 20 min at 140 000*g*. The concentration of S1 in the supernatant was determined using the Bradford assay. The values for the equilibrium dissociation constant (K_d) of S1 from actin were obtained by fitting the data to

$$S/A = [(A + S + K_d) - \{(A + S + K_d)^2 - 4AS\}^{1/2}]/2A \quad (1)$$

where S/A is the molar ratio of S1 bound to actin, and A and S are the total concentrations of actin and S1, respectively.

Mass Spectrometry. Modified S1 was obtained by incubating S1 (25 μM) in the presence of 1.0 mM MgADP and IAEDANS (1.0 mM) or pPDM (50 μM). After 15 min reactions at 4 °C, at least 90% of S1 was modified, as determined by the Ca^{2+}−ATPase activities. Unmodified and modified scallop S1 samples (2.0 mg/mL) were then digested with trypsin (1:200) for 15−20 min to produce a cut in loop 2 (*30*). After 10−15 min at 4 °C, the reactions were terminated with trypsin inhibitor (3-fold excess). The products of the limited tryptic digestion were separated by one-dimensional SDS polyacrylamide gel electrophoresis. The ~23 kDa protein band was excised and further digested in-gel with sequencing grade trypsin, following the method described previously (*31*). Molecular mass measurements were made by matrix-assisted laser desorption/ionization (MALDI). MALDI-MS employed a PerSeptive Voyager DE-

STR time-of-flight mass spectrometer (Applied Biosystems, Farmingham, MA). Sinapinic acid and α-cyano-4-hydroxycinnamic acid (HCCA) were employed as matrixes. Sinapinic acid was prepared as a saturated solution in 33% CH_3CN/67% H_2O/0.1% trifluoroacetic acid (TFA), while HCCA was saturated in 50%CH_3CN/50% H_2O/0.1% TFA. The sample (0.5 μL) was deposited on the sample plate, followed by an aliquot (0.5 μL) of matrix. Matrix and sample were briefly mixed and allowed to crystallize at room temperature, prior to their irradiation at 337 nm for mass analysis. The instrument was operated in linear mode to analyze peptides greater than 5 kDa in mass and in reflector mode to analyze smaller molecular weight peptides.

Peptide sequencing was accomplished by tandem mass spectrometry (MS/MS). Tryptic digests from the separated protein bands were loaded into nanoelectrospray (nano-ESI) tips (Protana, Odense, Denmark), and the tips were mounted into the ESI source. Tandem mass spectra were acquired with a quadrupole-time-of-flight mass spectrometer (QSTAR Pulsar-i, Applied Biosystems/MDS Sciex, Concord, Ontario, Canada).

RESULTS

Modification of Scallop and Skeletal S1. In previous studies, the reactivity of SH1 in skeletal S1 was shown to be influenced by both the nucleotide- and the actin-bound states of S1. In the presence of nucleotides, such as ADP and ATPγS, the rate of SH1 modification is increased, while actin inhibits this reaction (*32*−*34*). These changes in SH1 reactivity are correlated with similar changes in SH2 reactivity and SH1−SH2 cross-linking (*27*), and therefore, may be linked to the stabilization or destabilization of the SH1−SH2 helix. For scallop S1, several reagents were used to determine how different ligands affect the modification reaction. Figure 1 illustrates the effect of nucleotides (A) and actin (B) on the rate of NEM modification of scallop S1 by monitoring the changes in its EDTA−ATPase activity over reaction time. The upper plot (A) indicates that the addition of nucleotides increases the rate of NEM modification of scallop S1, with MgATPγS (▲) having a slightly larger effect than MgADP (■). The lower plot (B) shows the inhibition of the modification by actin (with the reactive Cys374 blocked by NEM) (◆) and in the post-hydrolysis state, mimicked by MgADP·V_i (▼). In these reactions, the EDTA−ATPase activity of scallop S1 decreases as the modification reaction progresses, which is similar to what is observed for thiol modifications in skeletal S1. The first-order rate constants for these modifications, obtained from the slopes of semilogarithmic plots similar to those shown in Figure 1, were determined for each ligand-bound state. The ratios of these rate constants (in the presence and absence of ligand) are presented in Table 1. These data show that the reactivity of the reactive thiol in the different states of scallop S1 decreases in the following order: S1ATPγS > S1ADP > S1 > S1-actin > S1ADPV_i. Similar results were also obtained with *N*-phenylmaleimide (data not shown). The above effects of nucleotides and actin on thiol modification in scallop S1 are qualitatively similar to their reported effects on SH1 labeling in skeletal S1 (*33*−*35*).

Importantly, the effect of NEM modification on the Ca^{2+}−ATPase activity of scallop S1 is different from that observed for skeletal S1. While the Ca^{2+}−ATPase activity is greatly enhanced upon modification of skeletal S1 by NEM, this activity does not change significantly with the modification of scallop S1. These differences are more apparent when the Ca^{2+}−ATPase activity is plotted against the EDTA−ATPase activity, which is equal to the percentage of unmodified S1. As normally observed in modifications of SH1 on skeletal S1 (*36*, *37*), there is a concomitant rise in Ca^{2+}−ATPase activity as the EDTA−ATPase activity decreases (in the presence and absence of MgADP) (Figure 2A). For scallop S1, such increases in the Ca^{2+}−ATPase activity are not observed upon thiol modification, when

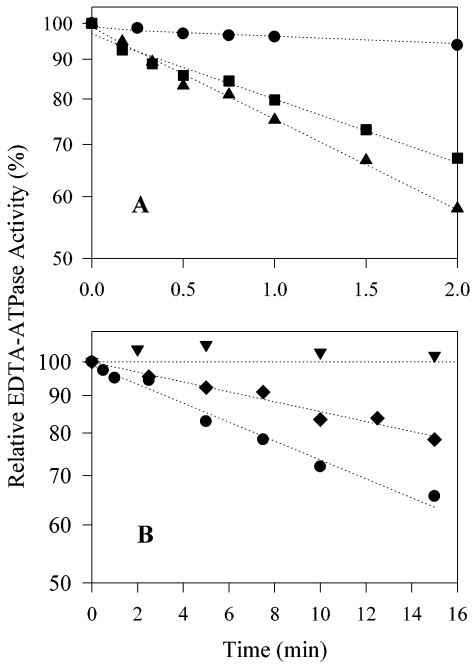

FIGURE 1: Effect of ligands on NEM modification of scallop S1. Semilogarithmic plots of the EDTA−ATPase activity versus modification time. (A) S1 (8.0 μM) was modified by NEM (32 μM) in the absence (●) and presence of 1.0 mM MgADP (■) or MgATPγS (▲) at 4 °C in the scallop S1 buffer (pH 7.0). (B) NEM modification of scallop S1 in the absence (●) or presence of 16 μM NEM-actin (◆) or the transition state analogue complex, MgADP·V_i (▼). The straight lines are the single-exponential fits of the relative EDTA−ATPase activities versus reaction time.

Table 1: Summary of Results Obtained from Modification Experiments[a]

ligand	k_L/k[b] (SH2 of scallop S1)
ADP	9 ± 1
ATPγS	14 ± 2
actin	0.5 ± 0.1
ADP·V_i	strongly inhibited[c]

[a] Prior to their modifications, scallop and skeletal S1 were incubated with either 1.0 mM nucleotide (MgADP or MgATPγS), the analogue transition complex (MgADP·V_i), or a 3-fold excess of actin (with Cys374 blocked by NEM). A 4-fold molar excess of NEM was added to S1 (pH 7.0 and 4 °C). The results are presented as ratios of the modification rates in the presence (k_L) and absence (k) of ligand. Each ratio is determined from the mean values of at least two independent experiments. [b] The rate of SH2 labeling (k) in scallop S1 in the absence of nucleotides was 0.022 ± 0.003 s^{-1}. [c] In certain cases (indicated strongly inhibited), the rate constant for the reaction in the presence of ligand could not be accurately determined because there was no measurable change in the EDTA−ATPase activity during the time course of the experiment.

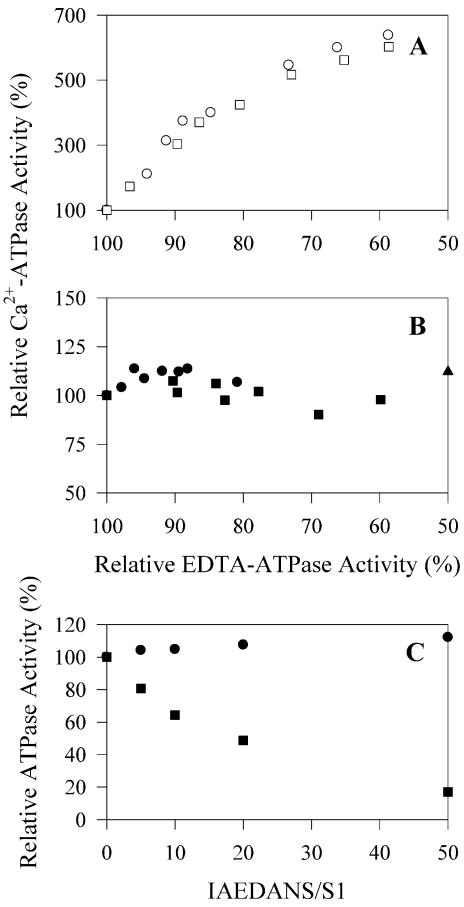

FIGURE 2: Monofunctional thiol modifications of skeletal (A) and scallop S1 (B and C). In time dependent reactions, a 4-fold molar excess of NEM (A and B) was added to S1 in both the absence (circles) or the presence of 1.0 mM MgADP (squares). Both ATPase activities were measured on the same time point aliquots of the S1 modification reaction. The activity results were normalized to the respective activities of unmodified S1. In fixed time reactions, different molar ratios of IAEDANS (C) were used to modify scallop S1·ADP (10 μM) for 10 min at 4 °C. The normalized Ca^{2+}- (●) and EDTA−ATPase (■) activities of S1 are plotted against the mole ratios of IAEDANS to S1. Reaction conditions (pH 7.0, 4 °C) are described in the Experimental Procedures.

monitored versus similar decreases in the EDTA−ATPase activity (Figure 2B). The addition of ADP to the scallop S1 reaction did not result in any change in this profile.

Scallop S1 was also modified with IAEDANS, a reagent shown to specifically label SH1 in skeletal S1. The IAEDANS modification was performed in the presence of ADP since the reaction was slow otherwise (data not shown). With increasing molar ratios of IAEDANS to scallop S1, the EDTA−ATPase activity of S1 decreased with very little change in the Ca^{2+}−ATPase activity (Figure 2C). In skeletal S1, such ATPase activity changes would be indicative of SH2 modification, not that of SH1. Reagents such as IANBD (4-[*N*-[(iodoacetoxy)ethyl]-*N*-methylamino]-7-nitrobenz-2-oxa-1,3-diazole) can be used under certain conditions to target SH2 modification in skeletal S1. These SH2-modified skeletal S1s have unchanged Ca^{2+}−ATPase and decreased EDTA−ATPase activities as compared to the unmodified S1 (*16*, *32*, *38*). Thus, the ATPase measurements of the modified scallop S1 suggest but do not prove that SH2, not SH1, is the more reactive group in this myosin.

Cross-Linking in the Nucleotide-Free State of Scallop and Skeletal S1. Four maleimide-based cross-linking reagents (oPDM, mPDM, pPDM, and BM) were utilized to compare the conformational dynamics of the SH1−SH2 helix in scallop and skeletal S1, but because of similar results data are shown for only two of these reagents. For skeletal S1, the results were similar to those reported previously (*32*). As shown for the pPDM reaction, the Ca^{2+}−ATPase activity of S1 initially increases, plateaus, and then begins to decrease, while the EDTA−ATPase activity decreases with the modification time (Figure 3A). Such ATPase changes are identified with the reagent first modifying SH1 and then, in a slower reaction, cross-linking to SH2. For scallop S1, the results of the modification reaction are different (Figure 3B). As seen from the EDTA−ATPase activities, the modification of the first group occurs much faster in scallop (by an order of magnitude) than skeletal S1, and it proceeds without any changes in the Ca^{2+}−ATPase of S1. Similar reaction profiles were also observed for the other reagents. As identified for the IAEDANS modification (see below), and indicated by the ATPase activity changes in Figure 3B, SH2 is the more reactive cysteine in scallop S1. Importantly, the pPDM attached to SH2 does not cross-link over a short time to SH1, as evident from the lack of decrease in the Ca^{2+}−ATPase activity (Figure 3B). Similar results were also observed for reactions with oPDM and mPDM (data not shown). BM, which has the longest cross-linking span, ∼15 Å, was able to cross-link the scallop S1 also in the absence of nucleotides, as deduced from the decrease in the Ca^{2+}−ATPase activity. Overall, these results indicate that the SH1−SH2 helix is stable in the nucleotide-free state of scallop S1 and that the SH1 and SH2 groups do not frequently approach closer than ∼12 Å of each other.

Cross-Linking in the Nucleotide-Bound States of Scallop and Skeletal S1. As observed in previous studies (*10*), the rate of SH1−SH2 cross-linking in skeletal S1 is strongly increased in the presence of MgADP (Figure 3C). This was also seen in the pPDM modification of scallop S1·MgADP (Figure 3D). However, unlike in skeletal S1, for which the cross-linking step is slower in most cases than the initial modification step, the cross-linking in scallop S1 is rate-limited by the initial modification reaction. This is evident from the similar rates of decrease in the Ca^{2+}− and EDTA−ATPase activities of S1 (Figure 3D). Such cross-linking kinetics precludes accurate measurements of the cross-linking rate constants. Similar results were also obtained using cross-linking reagents with longer (BM, data not shown) and shorter (oPDM—Figure 4A,B—and mPDM, data not shown) spans. In a previous study with skeletal S1, computer simulations were performed to estimate the lower limit constraints on the rate constants for SH1−SH2 cross-linking in S1·MgADP·V_i and S1·MgADP·AlF_4^-, for which the first step (SH1 modification) was not separated from the second one (cross-linking) (*39*). With this numerical analysis, lower limit values were also estimated for the cross-linking rate constants of the scallop S1 reactions in the presence of MgADP. For oPDM and pPDM, these lower limits were 3.75 and 15 min^{-1}, respectively. These lower limit cross-linking rates are much faster (between 200- and 300-fold) than the comparable reaction rates in skeletal S1 (0.013 and 0.070 min^{-1}, respectively; ref *39*).

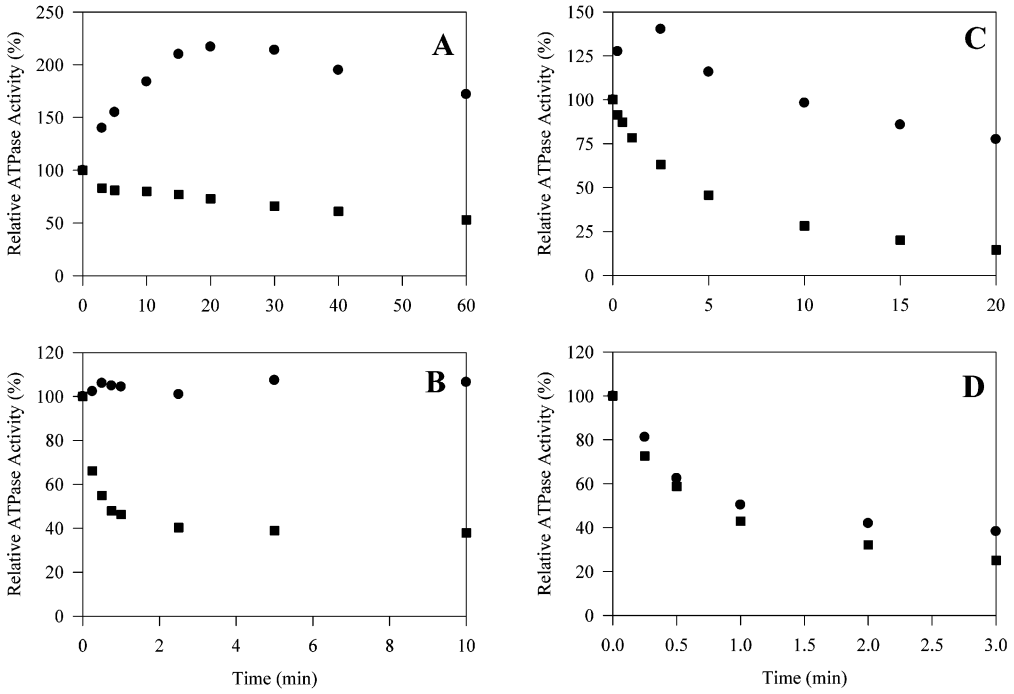

FIGURE 3: Time course of pPDM modifications of skeletal (A and C) and scallop (B and D) S1. S1 (12 μM) was modified with pPDM (18 μM) either in the absence (A and B) or presence of 1.0 mM MgADP (C and D). At selected time points, reaction aliquots were quenched with 1.0 mM DTT. The Ca^{2+}- (●) and EDTA−ATPase (■) activities were measured in representative reactions, normalized relative to the activities of unmodified S1, and plotted against the time of modification. Virtually identical results were obtained in modification reactions carried out on three different protein preparations. Reaction conditions (pH 7.0, 4 °C) are described in the Experimental Procedures.

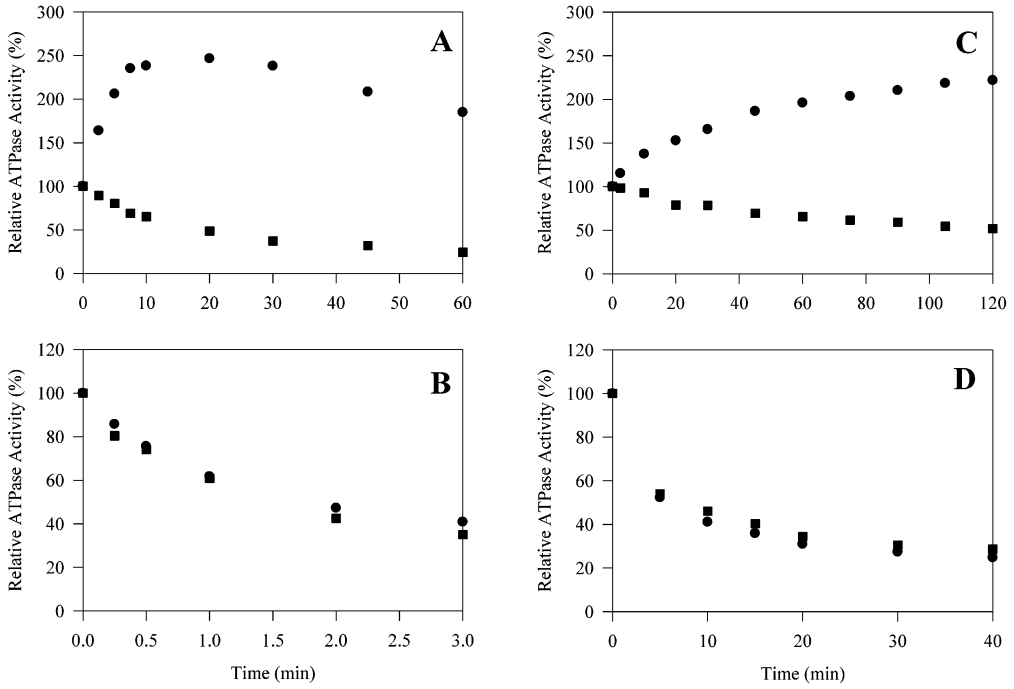

FIGURE 4: Time course of oPDM (A and B) and DTNB (C and D) modifications of skeletal (A and C) and scallop (B and D) S1 in the presence of 1.0 mM MgADP. S1 (10 μM) was modified with oPDM (15 μM) or DTNB (20 μM) at pH 7.0 and 4 °C. At selected time points, oPDM reaction aliquots were quenched with 1.0 mM DTT, while DTNB reaction aliquots were spun through a Sephadex G50 column to remove the excess of unreacted DTNB. The relative Ca^{2+}- (●) and EDTA−ATPase (■) activities of representative reactions are plotted against the time of modification. Each reaction was repeated at least three times, with similar results.

Because in contrast to skeletal S1 (Figure 4A), the cross-linking in scallop S1 occurred quickly (Figure 4B) with even the shortest reagent (oPDM, with a span of ~7−10 Å), we also examined the DTNB-mediated disulfide bond formation in S1. For skeletal S1·MgADP, disulfide bond formation is slow, occurring over a period of 24 h (*40*), and is not detected in the shorter time scale of our experiments (Figure 4C). For scallop S1·MgADP, as indicated by the ATPase measurements, the disulfide bond formation occurs quickly (Figure 4D), and the reaction is completed in less than 2 h (data not shown). Moreover, as in other cross-linking reactions, the disulfide cross-linking appears to be rate-

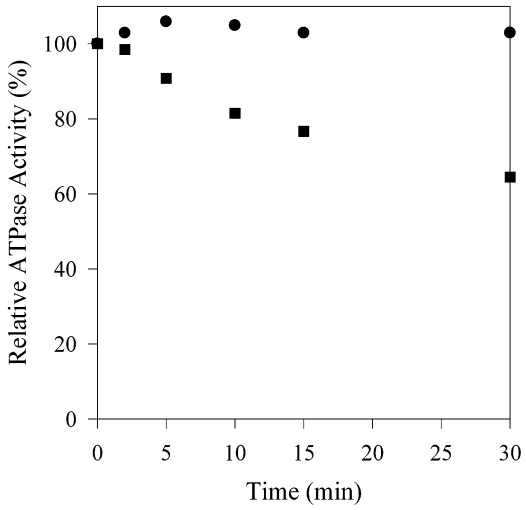

FIGURE 5: pPDM modification of scallop S1 in the presence of MgADP·V_i. S1 (10 μM) was modified with pPDM (15 μM) in the presence of MgADP·V_i at pH 7.0 and 4 °C. At selected time points, reactions in the aliquots were terminated with 1.0 mM DTT. The bound MgADP·V_i was released, as described in the Experimental Procedures, so that the Ca^{2+}- (●) and EDTA−ATPase (■) activities could be measured. Similar results were obtained in modifications of three independent S1 preparations.

limited by the initial reaction, the attachment of NTB to the reactive thiol.

The effects of different nucleotide states on the rate of cross-linking in scallop S1 were also examined. The pPDM modification reaction of scallop S1 occurs equally fast in both the MgADP and the MgATPγS states (data not shown). Because the overall reaction is rate-limited by the initial attachment of the reagent, differences in the rates of cross-linking between these states, if any, could not be determined. The results obtained for the MgADP·V_i state were strikingly different from those for the other two nucleotide states. The modification at the initial site was inhibited ~100-fold or more, and the subsequent cross-linking was inhibited to such an extent that in the time span of our experiments there was no measurable decrease in the Ca^{2+}−ATPase activity (Figure 5).

Mass Spectrometry of IAEDANS-Modified Scallop S1. To determine which thiol group, SH1 or SH2, is preferentially labeled in scallop S1, the sequence of this region was analyzed. In the case of skeletal S1, hydroxylamine can be used to cleave the Asn−Gly bond between the SH1 and the SH2 groups, producing two peptides that separate SH1 and SH2 (*41*). Similar hydroxylamine cleavage of scallop S1 produced several fragments, complicating the analysis of the reaction. Therefore, mass spectrometry was used to locate the site of thiol modification by IAEDANS.

To reduce the complexity of the MS analysis, unmodified and modified scallop S1 were cleaved with trypsin in a limited manner (i.e., at loop 2) producing the N-terminal ~72 kDa and C-terminal ~23 kDa fragments. Because loop 2 contains several lysine residues, all susceptible to trypsin, multiple C-terminal fragment lengths were observed (Figure 6B). The differences in these fragments correspond to various clips at the N-terminal K-K-G-K residues (residues 635−638). MALDI-MS of IAEDANS-modified sample revealed mass shifts confined to the C-terminal ~23 kDa fragment, spanning SH1 and SH2. These values correspond within an

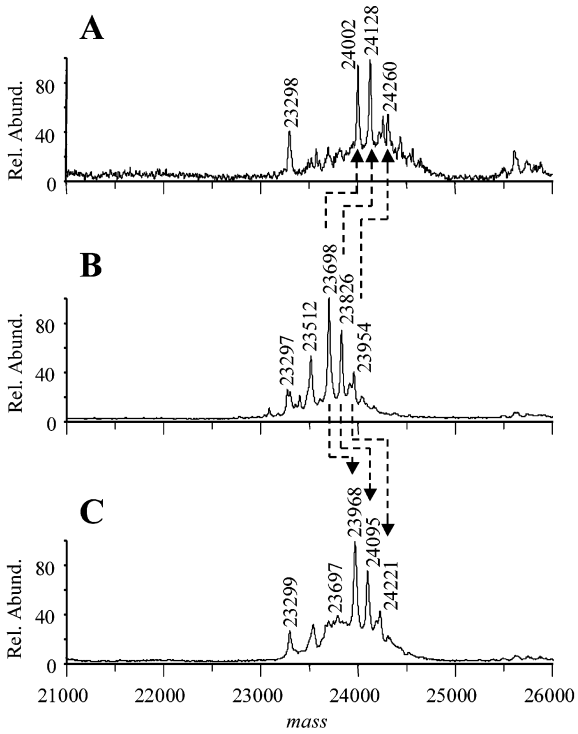

FIGURE 6: MALDI mass spectra of the C-terminal 23 kDa limited tryptic product of unmodified and modified scallop S1. (A) IAEDANS-modified sample; (B) unmodified sample; and (C) pPDM-modified sample. Because loop 2 of scallop S1 contains several lysine residues, the limited trypsin digestion produced several 23 kDa fragments. Differences in fragment masses are consistent with residues 635−638 of the scallop S1 sequence, corresponding to K-K-G-K. Within a mass accuracy of ±12 Da, the shifts in the masses of the 23 kDa fragment, indicated by the arrows, are due to addition of IAEDANS (306 Da) or pPDM (268 Da).

error of 0.05% (±12 Da for MALDI-MS experiments at a higher mass) to IAEDANS addition (Figure 6A) to the 23 kDa fragment.

Several cleavage sites for trypsin lie within the sequence of the C-terminal 23 kDa fragment, including one between SH1 and SH2. A complete in-gel tryptic digestion of this fragment was performed to localize the site of modification. The monoisotopic SH2 peptide ion is predicted at *m*/*z* 2601.4 Da, but the N-terminal glutamine can cyclize to pyroglutamic acid with consequent loss of 17 Da (theoretical $[M + H]^+$ at *m*/*z* of 2584.4). We found both forms of the SH2 peptide in our samples. Moreover, $[M + H]^+$ peaks at *m*/*z* 2907.4 and 2890.3 were unique to the IAEDANS-modified sample, corresponding to addition of IAEDANS to SH2 peptide (Figure 7A).

Peptide sequencing by electrospray ionization (ESI)-MS/MS of triply charged IAEDANS−SH2 peptide yielded primarily *y*-type products across an extensive span of the polypeptide and is consistent with monofunctional IAEDANS labeling at Cys693 of scallop S1 (Figure 8A).

The tryptic peptide containing SH1 (ICR) was not detected because of its small size. To assess the possibility of modifications of thiols other than SH2 (identified above), DTNB titration experiments were performed using IAEDANS-labeled scallop S1. The IAEDANS-modified S1, with a decrease of 80−90% of its EDTA ATPases, had approximately one less free cysteine group (13 ± 1) than the

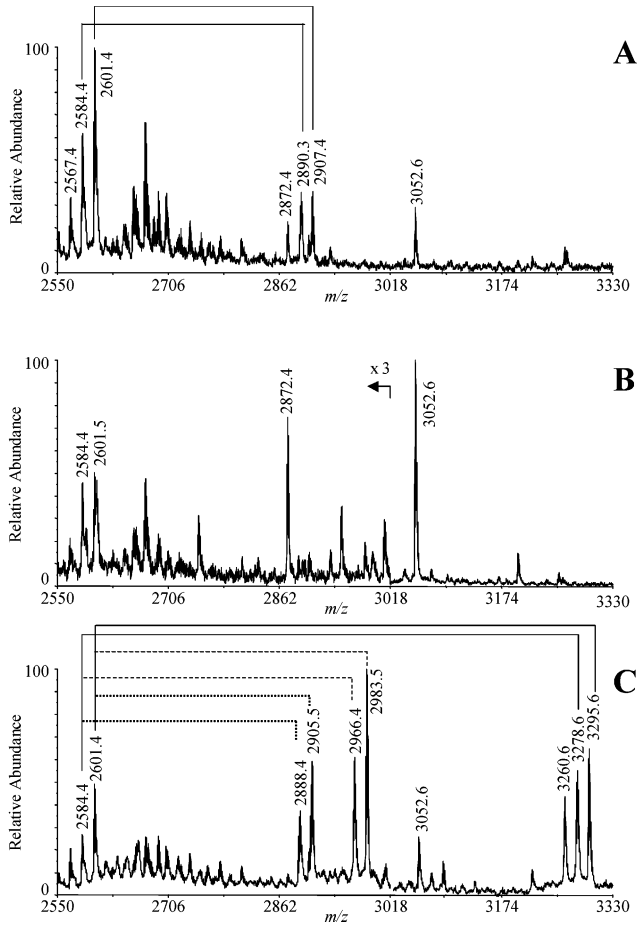

FIGURE 7: MALDI mass spectra of the complete tryptic digestion of the gel-isolated C-terminal 23 kDa tryptic peptide. (A) IAEDANS-modified sample; (B) unmodified sample; and (C) pPDM-modified sample. The N-terminal residue of the SH2 tryptic peptide is a Gln, which can cyclize to form pyro-Glu (having a decreased mass of 17 Da). Both forms of this peptide are present (monoisotopic $[M + H]^+$ ions observed at *m*/*z* 2601.4 and 2584.4). IAEDANS modification of the SH2 peptide leads to the mass observed at *m*/*z* 2907.4 (and *m*/*z* 2890.3 for the pyro-Glu form). The monofunctional pPDM modification of the SH2 peptide leads to the ion observed at *m*/*z* 2905.5 (and *m*/*z* 2888.4, the pyro-Glu form). The SH1−SH2 cross-linked peptides are observed at *m*/*z* 3295.6 (and *m*/*z* 3278.6). The other set of peaks at *m*/*z* 2983.5 (and *m*/*z* 2966.4) also derive from pPDM-modified SH2 but with an additional mass of 78 Da, postulated to arise from β-mercaptoethanol addition to pPDM's second maleimide.

unmodified scallop S1 (14 ± 1). Thus, the combination of the mass spectrometry, ATPase activities, and DTNB titrations allows us to conclude that the label is reacting specifically with SH2.

Mass Spectrometric Identification of pPDM Cross-Linked Residues. In skeletal S1, SH2 has been shown to cross-link to groups other than SH1. For example, with SH1 blocked, pPDM can cross-link SH2 to Cys540 (*42*). It has also been shown that at least one reagent (dibromobimane, DBB) cross-links from SH1 to Cys522 and not to SH2 (*43*). In principle, pPDM may cross-link also from a cysteine to a lysine group, as seen in skeletal α-actin at pH 9 (*44*). Such a pPDM cross-link between SH2 and a nearby lysine group has been identified in a crystal structure of the cross-linked scallop S1 (*9*). Because of these different cross-linking possibilities, mass spectrometry was employed to identify the cross-linked sites on scallop S1. Limited tryptic digestions of cross-linked scallop S1 yielded the same products, with quantities of the ~23 kDa fragment similar to those obtained from unmodified S1. This result confines the cross-linking to the three cysteine-containing C-terminal 23 kDa fragments (SDS PAGE data not shown). Moreover, DTNB titration of scallop S1 almost completely cross-linked by pPDM revealed a loss of approximately two cysteine groups in samples, verifying cross-linking of SH2 to SH1.

The added mass of pPDM to a peptide fragment was calculated to be 268 Da (if the maleimide rings are not hydrolyzed) or 304 Da (both maleimide rings hydrolyzed (*44*)). As compared to unmodified S1, MALDI-MS of the pPDM-modified sample revealed a 269 shift for the C-terminal ~23 kDa fragment (Figure 6C). Because all reactions were performed at pH 7.0 and analyzed soon after, hydrolysis of the maleimide rings, which occurs slowly at pH 7.0, was not observed.

To localize the pPDM cross-link further, the 23 kDa fragment was digested in-gel with trypsin. Cleavage products were extracted from the gel and analyzed by MALDI-MS. The 23 kDa fragment contains three Cys residues as well as Lys705, which was identified as cross-linked by crystallography. Theoretical masses of scallop S1 tryptic peptides with assorted cross-links are listed in Table 2. By comparing mass spectra of unmodified (Figure 7B) and pPDM-modified samples (Figure 7C), it is evident that new peaks are present in the modified sample. Each sample revealed two forms of the SH2 tryptic peptides, with the N-terminal Gln and cyclized pyro-Glu (differing by 17 Da, see above). A comparison of new peaks with the theoretical masses for the tryptic peptide ions that might be generated from pPDM-labeled S1 indicates monofunctional attachment of pPDM to the SH2 peptide (observed $[M + H]^+$ ions at *m*/*z* 2905.5 and 2888.4) and bifunctional attachment of pPDM to the SH1 and SH2 peptides (observed $[M + H]^+$ ions of *m*/*z* 3295 and 3278). The peaks at *m*/*z* 2983.5 and 2966.4 correspond to pPDM-modified SH2 peptide with 78 Da additional mass, possibly from β-mercaptoethanol addition to pPDM. MS/MS data support a 78 Da adduct to pPDM. Detecting monofunctionally modified SH2 suggests that the cross-link initiates from pPDM attachment to the SH2 thiol and is completed by bridging to SH1. This sequence of reactions is suggested also by results from ATPase assays of the cross-linking reaction (Figure 3B). The crystal structure of the pPDM cross-linked scallop S1 implies, as well, that the cross-linking starts from SH2, but it terminates at K705 (*9*).

Sequencing of the pPDM cross-linked SH1−SH2 peptide by ESI-MS/MS yielded primarily *y*-type products across an extensive span of the polypeptide and was consistent with the bifunctional label binding at Cys703 and Cys693 (Figure 8B). These pPDM-related ions revealed that both maleimide rings could hydrolyze under the conditions employed. Singly hydrolyzed pQ-SH2-pPDM-S1 is also evident from its monoisotopic $[M + H]^+$ ion observed at *m*/*z* 3260.6. Moreover, the isotope profile (data not shown) of doubly hydrolyzed pQ-SH2-pPDM-S1 reveals an unexpected ion at *m*/*z* 3277.5, one *m*/*z* lower than the peptide's monoisotopic ion and insufficiently abundant to ascribe to the doubly hydrolyzed pQ-SH2-pPDM-S1 isotope profile. We attribute it to singly hydrolyzed SH2-pPDM-S1. A low abundance ion was similarly observed at *m*/*z* 2965.3, one *m*/*z* below

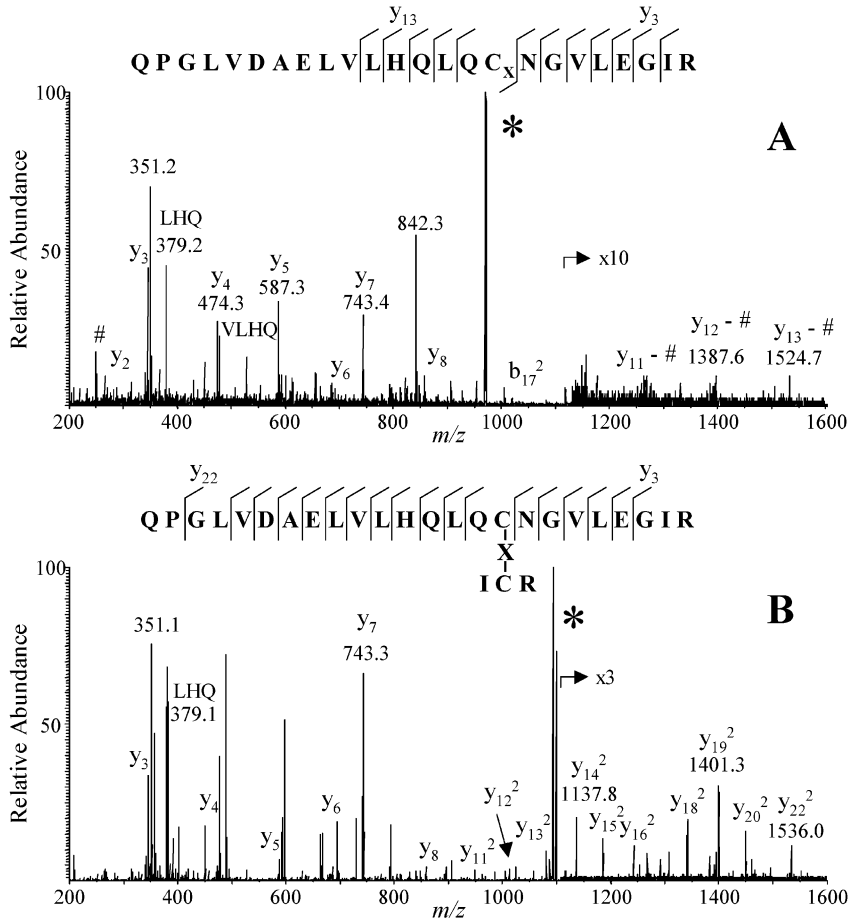

FIGURE 8: MS-peptide sequencing of the modified and cross-linked peptides. (A) ESI-MS/MS spectrum of the $(M + 3H)^{3+}$. IAEDANS-peptide at *m*/*z* 970.4. Extensive 1^+- and 2^+-charged *y*-type product ions were generated from dissociation of the 3^+-charged precursor ion. (Nomenclature used for the oligopeptide fragmentation pattern is based on conventional notation. Subscripts are used to denote the residue position, counting from the N-terminus for a_n, b_n, and c_n ions and from the C-terminus for x_n, y_n, and z_n products. A superscript is added to indicate the product ion charge state. Lack of a superscript denotes a singly charged fragment ion.) The precursor ion is labeled with the * symbol. For the IAEDANS-peptide, a fragmentation of the label molecule was also observed [e.g., the $(y_{11} - \#)$ ion denotes the y_{11} product and cleavage of the label at the $-CH_2-NH-$ bond to lose 249 Da. Cleavage of the label is indicated also by the ion at *m*/*z* 249 (# symbol).]. Two other internal fragments (VLHQ and LHQ) were also detected and are indicated in the figure. The fragmentation pattern is consistent with the label residing on SH2 (Cys693). (B) ESI-MS/MS spectrum of the $(M + 3H)^{3+}$ of the pPDM cross-linked tryptic peptides at *m*/*z* 1099.2. For the pPDM cross-linked peptide, similar MS/MS data was obtained from the 4^+-charged precursor ion at *m*/*z* 824.7 (data not shown). The fragmentation pattern is consistent with the pPDM label spanning cysteine residues 693 and 703.

the putative pQ-SH2-pPDM-β-ME monoisotopic ion, and is similarly ascribed to singly hydrolyzed SH2-pPDM-β-ME.

Because X-ray structure analysis identified Lys705 rather than SH1 as the residue cross-linked by pPDM to SH2, we examined by mass spectrometry also the cross-linked S1 from the same stock that was used for crystal growth in the study of Himmel et al. (*9*). The sample employed for crystal growth revealed $[M + H]^+$ ions characteristic of uncross-linked SH2 peptide at *m*/*z* 2601.3 and 2584.3 (pyroGlu-form) and of the SH2−SH1 cross-linked peptides at *m*/*z* 3295.3 and 3278.3. Additional ions corresponding to pPDM monofunctionally cross-linked to SH2 ($[M + H]^+ = m/z$ 2905.3 and 2888.3) and the putative SH2-pPDM-β-mercaptoethanol species ($[M + H]^+ = m/z$ 2983.3 and 2966.3) were also observed. However, peaks consistent with an SH2-pPDM-Lys705 tryptic peptide (monoisotopic $[M + H]^+$ ions expected at *m*/*z* 3595.8 and 3578.8) were not seen. Tryptic peptides from the crystal growth sample were also evaluated by LC-ESI-MS/MS, seeking evidence for the 3.6 kDa peptides, but neither was observed. On the basis of these data, we estimate that an SH2-pPDM-Lys705 species, if present, can account for no more than 5−10% of the cross-linked material.

Actin Binding Properties of Cross-Linked Scallop S1. It is well-established that the binding to actin of SH1−SH2 cross-linked skeletal S1 is much weaker than that of unmodified S1 and is similar to that of the weak-binding state of S1. For unmodified scallop S1, the K_d value obtained for the S1·ADP state was 0.5 ± 0.1 μM. For cross-linked (and disulfide-bonded) scallop S1, the K_d values could not be accurately determined. Complicating these measurements was the higher ionic strength of the buffer solution, containing 100 mM NaCl to stabilize the scallop S1. The K_d values ranged between 200 and 300 μM, similar to those obtained with scallop S1·ADP·BeF_x, the transition-state analogue of the S1·ATP state. Thus, SH1−SH2 cross-linking of scallop S1 also results in the weakening of the S1 binding to actin.

DISCUSSION

The crystal structure of chicken skeletal S1 showed that the SH1 and SH2 groups are located ~19 Å apart on a bent

Table 2: Possible Cross-Linked Peptides that Could Be Generated from the Complete Tryptic Digestion of the 23 kDa Fragment

tryptic fragment	theoretical monoisotopic mass[a] (Da)	theoretical mass for pyro-Glu modification[b] (Da)
Unmodified peptide		
678−701 (contains SH2)	2601.4	2584.4
702−704 (contains SH1)	391.2	
670−677 (contains Cys670)	929.5	
705−710 (contains Lys705)	691.4	
Cross-linked peptides[c]		
SH2-pPDM-SH1	3295.6	3278.6
SH2-pPDM-Cys670	3833.9	3816.9
SH1-pPDM-Cys670	1623.7	
SH2-pPDM-Lys705	3595.8	3578.8

[a] The theoretical monoisotopic masses of the $[M + H]^+$ species were determined from the Peptide Mass program, which is available from the ExPASy (Expert Protein Analysis System) proteomics server (us.expasy.org). [b] The pyro-Glu modification occurs when an N-terminal Gln residue is cyclized (decrease in peptide mass of 17 Da). Of the tryptic peptides listed in the table, only the SH2-containing peptide has an N-terminal Gln group. [c] The cross-linked peptides represent all possible combinations of the SH1-, SH2-, and Cys670-containing peptides. Because of the atomic structure of scallop pPDM-S1·ADP, the peptide containing SH2-Lys705 was also considered.

α-helix (*1*). Several subsequently solved structures of nucleotide-bound states of S1 from *Dictyostelium discoideum* and smooth muscle S1 (*2*, *4*, *6*) showed a rigid conformation for the SH1−SH2 helix, which is in contrast with the results obtained from solution studies. In particular, recent kinetic studies of SH1−SH2 cross-linking in skeletal S1 suggested that this helix changes throughout the ATPase cycle; it is destabilized in the S1·ADP, S1·ATPγS, and S1·ADP·BeF_x complexes and stabilized in the acto-S1 complexes (*27*, *39*, *45*). In line with these results, recent crystallographic work provided evidence for the unwinding of the SH1−SH2 helix in the atomic structures of scallop S1·ADP, S1·AMPPNP, and S1·ADP·BeF_x (*7*, *9*). However, the crystallographic mapping of the pPDM cross-linking in scallop S1 to SH2 and Lys705, but not to SH1, is unexpected in view of the well-established reactivity of SH1 in skeletal S1 (*9*). Because of this, but mainly to obtain the missing information on the dynamics of the SH1−SH2 helix in scallop S1 in solution, we investigated the labeling and cross-linking of this helix.

Reactive Cysteines in Skeletal and Scallop S1. Our results with monofunctional reagents have shown both important differences and similarities between the local environments of the SH1 and SH2 groups in skeletal and scallop S1. The main difference between these S1 isoforms is the change in the reactivities of the SH1 and SH2 thiols. With scallop S1, the results of the modification experiments, combined with mass spectrometry, showed that SH2 is the more reactive sulfhydryl. This was true for both iodo-based (IAEDANS) and maleimide-based (NEM, pPDM) reagents, suggesting that the general accessibility of SH1 and SH2 to modifications is different in scallop S1 as compared to skeletal S1. These results are consistent with crystal structures of the internally-uncoupled scallop S1, in which only SH2 is chemically modified by pPDM, but SH1 does not participate in the cross-linking (*9*).

Despite this reactivity switch in skeletal and scallop S1, the effects of ligands on their reactivities are similar for both S1 isoforms. The modification of SH2 (and of SH1 in skeletal S1) is accelerated in the presence of MgADP and even more in the presence of MgATPγS. Correspondingly, the MgADP structure of scallop S1 shows that there are significant differences in the SH1−SH2 helix region as compared with the nucleotide-free state. The portion of the helix containing SH1 is disordered, so that it is not possible to determine the exact position of SH1. In parallel, the contacts between SH2 and residues in the 50 kDa domain are broken, and this thiol becomes more exposed (*7*, *8*). In solution, neither group is modified readily in this state, in agreement with the crystallographic evidence. The inhibition by actin of SH2 labeling in scallop S1 and SH1 labeling in skeletal S1 (*46*) is also similar. These similarities suggest that the bound nucleotides and actin alter the conformation of the entire SH1−SH2 helix and not just the local environment of SH1 or SH2.

We used chemical cross-linking to examine the dynamics of the SH1−SH2 helix in scallop myosin. Mass spectrometry mapped the pPDM cross-linking in scallop S1 to SH2 and SH1. The preferential cross-linking of SH2 to SH1 was suggested also by the DTNB-mediated disulfide formation in scallop S1. In contrast, in the crystal structure of pPDM cross-linked scallop S1·ADP, the bridging of pPDM occurs from SH2 to Lys705, adjacent to SH1 (*9*). The different assignments of the residue cross-linked to SH2 do not stem from experimental differences, as the mass spectrometry analysis was done also on S1 samples taken from the stocks that were used for crystal growth. It is possible that both cross-linkings occur in solution, but only the SH2−Lys705 cross-linked S1 crystallizes under the previously used conditions (*9*). To escape detection by MALDI and ESI mass spectrometry, this S1 must be much less abundant (<10%) than the SH1−SH2 cross-linked S1. It is also possible that crystallization selects the small fraction of S1 with pPDM tethered only to SH2 and extending to Lys705 but not bound to it. Such a possibility would be consistent with our mass spectrometry results, and it might be difficult to assess the presence or absence of a chemical bond to Lys705 at the reported resolution of the X-ray study (*9*).

The main conclusion drawn from the cross-linking experiments is that the dynamics of the SH1−SH2 helix in scallop S1 is significantly different from that in skeletal S1. MgADP induced a greater destabilization of the SH1−SH2 helix in scallop S1 than in skeletal S1. This effect is most evident in the cross-linking reactions with the short-span reagents, oPDM and DTNB, which cross-link skeletal S1 at a slow rate. In scallop S1, the reaction with oPDM and the longer reagents occurred at similar time scales, and the disulfide bond formation was completed in 2 h (vs >24 h in skeletal S1). This suggests that the probability of SH1−SH2 helix melting is much greater in scallop than in skeletal S1. In contrast to skeletal S1 for which MgATPγS induced a somewhat greater destabilization of the SH1−SH2 helix than MgADP, we could not differentiate between the cross-linking of these two states of the scallop S1 helix. Such small differences between ADP and ATPγS are consistent with the ability of the nucleotide pocket of S1 to accommodate either ADP or ATP in the same structure (*4*, *5*, *7*), and/or crystallize in the S1·ATP state with ADP bound in the pocket (*7*). Thus, the conclusion derived from structural studies that these nucleotide states are easily convertible and are sepa-

rated by a low energy barrier is supported by the results of solution cross-linking experiments.

Stability of the SH1−SH2 Helix in Solution and in Atomic Structure. The finding that the SH1−SH2 helix can be cross-linked by short reagents in solution is perhaps the earliest evidence of a well-defined nucleotide dependent structural change in the myosin head (*32*). Cross-linking experiments on skeletal myosin indicated that the SH1−SH2 helix is unwound in the presence of nucleotides (*11*). Nevertheless, the atomic structures of a methylated chicken S1 in the apo state, and of *Dictyostelium* motor domains in the presence of ATP analogues, contained an intact SH1−SH2 helix (*1*, *2*, *4*, *5*). The SH1−SH2 helix was also preserved in the transition state induced by MgADP·AlF_4^- or MgADP·V_i in the *Dictyostelium* motor domain and in the chicken smooth muscle motor domain-essential light chain complex (*2*, *3*). In the atomic structure of scallop S1, the SH1−SH2 helix also remained intact in nucleotide-free and in transition states (*8*). In contrast, the SH1−SH2 helix is melted in the MgADP state, when scallop S1 is complexed with Mg·ATP analogues (MgAMPPNP and MgADP·BeF_x), and in the pPDM cross-linked MgADP and MgATPγS structures (*7*, *9*). The difference between scallop S1 and *Dictyostelium* motor domain structures is restricted therefore to the internally uncoupled conformation when ATP analogues or MgADP occupy the active site. The main factor favoring the demonstration of SH1−SH2 helix melting in scallop S1 may be its less stable structure (as indicated by much faster cross-linking than in skeletal S1), possibly more suitable for trapping the unwound SH1−SH2 conformation. The intact myosin of *Dictyostelium*, mutated to contain a cysteine in position of rabbit skeletal SH1, is cross-linked by pPDM, indicating that the unwinding of the SH1 helix occurs also in this myosin (*46*). However, all structures with ADP and ATP analogues were obtained with truncated *Dictyostelium* constructs. Solution studies have shown that the modification of SH2 is decreased and thus, the stability of the SH1−SH2 helix is increased by the truncation (*47*). The determination of the crystal structure of the full-length *Dictyostelium* S1 will be needed to reconcile it with the results of cross-linking studies.

It is noteworthy that so far, scallop S1 is the only isoform for which cross-linking studies agree with the results of crystallography regarding the conditions at which the SH1−SH2 helix is unwound. The discrepancy about the cross-linking of SH2 to SH1 (this paper) or K705 (*9*) is less significant and does not affect the conclusions on the helix dynamics. Overall, our results show that the SH1−SH2 helix in scallop S1 is more dynamic than that in skeletal S1. Although the amino acid sequence between SH1 and SH2 is identical, the sequence flanking SH1 and SH2 shows several differences. The contacts that these flanking regions make with other regions of S1 (i.e., the relay helix) may influence the stability of the SH1−SH2 helix and produce isoform-specific differences in the rate and extent to which different nucleotide states destabilize this helix in different myosins. Despite such differences, the examples of skeletal and scallop S1 suggest that the destabilization of the SH−SH2 helix is an integral part of the ATPase cycle of myosin. Structural studies indicate that the intact SH1−SH2 helix serves as a clutch that couples the active site with the converter and that the melting of the helix results in an internally uncoupled ATP state that follows the dissociation of myosin from actin (*9*).

REFERENCES

1. Rayment, I., Rypniewski, W. R., Schmidt-Bäse, K., Smith, R., Tomchick, D. R., Benning, M. M., Winkelmann, D. A., Wesenberg, G., and Holden, H. M. (1993) *Science 261*, 50−8.
2. Fisher, A. J., Smith, C. A., Thoden, J. B., Smith, R., Sutoh, K., Holden, H. M., and Rayment, I. (1995) *Biochemistry 34*, 8960−72.
3. Smith, C. A., and Rayment, I. (1996) *Biochemistry 35*, 5404−17.
4. Gulick, A. M., Bauer, C. B., Thoden, J. B., and Rayment, I. (1997) *Biochemistry 36*, 11619−28.
5. Bauer, C. B., Holden, H. M., Thoden, J. B., Smith, R., and Rayment, I. (2000) *J. Biol. Chem. 275*, 38494−9.
6. Dominguez, R., Freyzon, Y., Trybus, K. M., and Cohen, C. (1998) *Cell 94*, 559−71.
7. Houdusse, A., Kalabokis, V. N., Himmel, D., Szent-Györgyi, A. G., and Cohen, C. (1999) *Cell 97*, 459−70.
8. Houdusse, A., Szent-Györgyi, A. G., and Cohen, C. (2000) *Proc. Natl. Acad. Sci. U.S.A. 97*, 11238−43.
9. Himmel, D. M., Gourinath, S., Reshetnikova, L., Shen, Y., Szent-Györgyi, A. G., and Cohen, C. (2002) *Proc. Natl. Acad. Sci. U.S.A. 99*, 12645−50.
10. Burke, M., and Reisler, E. (1977) *Biochemistry 16*, 5559−63.
11. Wells, J. A., Knoeber, C., Sheldon, M. C., Werber, M. M., and Yount, R. G. (1980) *J. Biol. Chem. 255*, 11135−40.
12. Thomas, D. D., and Cooke, R. (1980) *Biophys. J. 32*, 891−906.
13. Barnett, V. A., and Thomas, D. D. (1987) *Biochemistry 26*, 314−23.
14. Kinose, F., Wang, S. X., Kidambi, U. S., Moncman, C. L., and Winkelmann, D. A. (1996) *J. Cell. Biol. 134*, 895−909.
15. Patterson, B., Ruppel, K. M., Wu, Y., and Spudich, J. A. (1997) *J. Biol. Chem. 272*, 27612−7.
16. Root, D. D., and Reisler, E. (1992) *Biophys. J. 63*, 730−40.
17. Marriott, G., and Heidecker, M. (1996) *Biochemistry 35*, 3170−4.
18. Bobkov, A. A., Bobkova, E. A., Homsher, E., and Reisler, E. (1997) *Biochemistry 36*, 7733−8.
19. Bobkova, E. A., Bobkov, A. A., Levitsky, D. I., and Reisler, E. (1999) *Biophys. J. 76*, 1001−7.
20. Godfrey, J. E., and Harrington, W. F. (1970) *Biochemistry 9*, 886−93.
21. Spudich, J. A., and Watt, S. (1971) *J. Biol. Chem. 246*, 4866−71.
22. Weeds, A. G., and Pope, B. (1977) *J. Mol. Biol. 111*, 129−57.
23. Lehrer, S. S., Nagy, B., and Gergely, J. (1972) *Arch. Biochem. Biophys. 150*, 164−74.
24. Stafford, W. F., Szentkiralyi, E. M., and Szent-Györgyi, A. G. (1979) *Biochemistry 18*, 5273−80.
25. Kalabokis, V. N., and Szent-Györgyi, A. G. (1997) *Biochemistry 36*, 15834−40.
26. Stafford, W. F., Jacobsen, M. P., Woodhead, J., Craig, R., O'Neall-Hennessey, E., and Szent-Györgyi, A. G. (2001) *J. Mol. Biol. 307*, 137−47.
27. Nitao, L. K., and Reisler, E. (1998) *Biochemistry 37*, 16704−10.
28. Bradford, M. M. (1976) *Anal. Biochem 72*, 248−54.
29. Ellman, G. L. (1959) *Arch. Biochem. Biophys. 82*, 70−77.
30. Szentkiralyi, E. M. (1984) *J. Muscle Res. Cell Motil. 5*, 147−64.
31. Shevchenko, A., Wilm, M., Vorm, O., and Mann, M. (1996) *Anal. Chem 68*, 850−8.
32. Reisler, E., Burke, M., Himmelfarb, S., and Harrington, W. F. (1974) *Biochemistry 13*, 3837−40.
33. Polosukhina, K., and Highsmith, S. (1997) *Biochemistry 36*, 11952−8.
34. Hiratsuka, Y., Eto, M., Yazawa, M., and Morita, F. (1998) *J. Biochem. 124*, 609−14.
35. Phan, B. C., Peyser, Y. M., Reisler, E., and Muhlrad, A. (1997) *Eur. J. Biochem. 243*, 636−42.
36. Sekine, T., and Kielley, W. W. (1964) *Biochim. Biophys. Acta 81*, 336.
37. Crowder, M. S., and Cooke, R. (1984) *J. Muscle Res. Cell Motil. 5*, 131−46.
38. Ajtai, K., and Burghardt, T. P. (1989) *Biochemistry 28*, 2204−10.
39. Nitao, L. K., Yeates, T. O., and Reisler, E. (2002) *Biophys. J. 83*, 2733−41.
40. Wells, J. A., and Yount, R. G. (1980) *Biochemistry 19*, 1711−7.

41. Sutoh, K. (1981) *Biochemistry 20*, 3281−5.
42. Chaussepied, P., Mornet, D., and Kassab, R. (1986) *Proc. Natl. Acad. Sci. U.S.A. 83*, 2037−41.
43. Ue, K. (1987) *Biochemistry 26*, 1889−94.
44. Knight, P., and Offer, G. (1978) *Biochem. J. 175*, 1023−32.
45. Nitao, L. K., and Reisler, E. (2000) *Biophys. J. 78*, 3072−80.
46. Liang, W., and Spudich, J. A. (1998) *Proc. Natl. Acad. Sci. U.S.A. 95*, 12844−7.
47. Reynoso, J. R., Jr., Bobkov, A., Muhlrad, A., and Reisler, E. (2001) *J. Muscle Res. Cell Motil. 22*, 657−64.

BI027312U